American Journal of Pathology, Vol. 135, No. 4, October 1989

Primary Polyoma Virus-Induced Murine Thymic Epithelial Tumors

A Tumor Model of Thymus Physiology

Glenn P. Hoot and John R. Kettman
From the Department of Microbiology, University of Texas Southwestern Medical Center at Dallas, Dallas, Texas

Thymic tumors were induced in C3H/Bittner mice by neonatal inoculation with polyoma virus. The objective of this study was to identify the phenotypes of the cells within the tumors and to attempt to determine the origin of the neoplastic cell population(s). At the ultrastructural level, the neoplastic cells resembled normal thymic epithelium with tonofilaments and desmosomes. Immunoperoxidase staining demonstrated the presence of cytokeratin, Ia^k, β_2-microglobulin, asialo-GM_1, the thymic cortical epithelial marker ER-TR4, and the medullary epithelial marker ER-TR5. Islands of normal cortical thymocytes supported by residual normal cortical epithelium and acid phosphatase-positive cortical macrophages were interspersed in the tumors. Residual islands of normal medullary architecture with nonspecific esterase-positive IDCs were rarely identified in tumors. Most lymphocytes in the tumors were normal immature cortical thymocytes with the phenotype Tdt^+, PNA^+, $Thy1.2^{brigbt}$, $Ly\text{-}1^{dull}$, $H\text{-}2K^{k\ dull}$, ThB^+, $J11d^+$, and $Lyt\text{-}2^+L3T4^+$. Lymphocytes in the tumors were steroid-sensitive like normal thymocytes. The proportions of $Lyt\text{-}2^+L3T4^-$ and $Lyt\text{-}2^-L3T4^+$ cells were generally larger in the tumors than in normal thymus and reflected the higher frequency of lymphocytes in the tumors capable of proliferating* in vitro *in response to Con A plus IL-2. The data were consistent with the hypothesis that the neoplasia originates from thymic epithelium that is interspersed with normal, developing thymic lymphocytes. (Am J Pathol 1989, 135:679–695)

The thymus, composed of both lymphoid and nonlymphoid cells, is the primary lymphoid organ in which early T cell developmental events take place. The nonlymphoid elements, ie, epithelial cells, cortical macrophages, and medullary interdigitating cells (IDCs), are involved in establishing intrathymic microenvironments. In these microenvironments, thymocytes proliferate, express clonal diversity, differentiate, and are subjected to clonal selective pressures to give rise eventually to a pool of emigrants capable of establishing the peripheral mature T cell compartment.[1–11] The architectural organization of the thymus is believed to orchestrate the sequence of intrathymic developmental events.[12–17]

An approach to understanding thymic microenvironments might be to unravel the architectural complexity. Both naturally occurring and experimentally induced thymic epithelial tumors were used as models for dissecting intrathymic lymphocyte maturation steps.[18–28] Disruption of thymic stromal architecture by neoplastic progression can conceivably have an effect on thymocyte development. (Note: The term *thymoma* is used frequently, but perhaps inappropriately, to describe thymic tumors in which the lymphoid component of the thymus is neoplastic. These types of tumors should be described as thymic lymphomas or thymic leukemias, whereas the term *thymoma* should be reserved for those tumors in which the thymic epithelial component gives rise to the tumor. Although the tumors used in this study are true thymomas, we refrained from using this term because its application to a variety of cytologically and biologically different neoplasms has led to confusion.[18])

We studied an *in vivo* tumor model, in which neonatal C3H/Bittner mice injected with the PTA-5 strain of polyoma (Py) virus develop epithelial tumors.[29–32] The efficiency of thymic tumor induction is high. Data are presented here regarding the histology of these primary thymic tumors and the phenotype of the thymocytes contained within the epithelial tumors.

This work was supported by National Cancer Institute grant #1-R01-CA-41679-01, grant 5-P01-AI-11851-14, and NCI Cancer Immunology Training grant 5-T32-CA-09082.

Accepted for publication June 12, 1989.

Address reprint requests to John R. Kettman, PhD, Department of Microbiology, University of Texas Southwestern Medical Center at Dallas, 5323 Harry Hines Boulevard, Dallas, TX 75235-9048.

Materials and Methods

Animals and Tumor Induction

C3H/Bittner mice, originally obtained from Dr. B. Amos, Duke University Medical School, were bred at our institution. Neonates aged 1-2 days old were reared in isolation from the main breeding colony once injected subcutaneously with 50 μl of a stock of Py virus, which had been titered in a plaque-forming assay, on NIH 3T3 monolayers, at 10^8 to 10^9 PFU/ml after 10 days. The seed virus stock, 2PTA-5, was an uncloned fifth serial passage in $P388D_1$ cells, of a wild-type Py virus provided by Dr. C. J. Dawe, Harvard Medical School.[32]

Steroid-Induced Acute Thymic Involution

Acute thymic involution was induced by injecting each animal intraperitoneally with 4 mg of hydrocortisone (Sigma Chemical Co., St. Louis, MO) emulsified in 0.5 ml of corn oil.

Preparation of Cells for Flow Cytometry

Cell suspensions were obtained by pressing tissue through a 40-mesh wire screen (Thomas Scientific, Swedesboro, NJ). Debris was removed after settling for 10 minutes at 1*g*, the suspension was pelleted and treated with ammonium chloride-TRIS for 1 minute to lyse erythrocytes, after which it was washed twice in cold RPMI 1640.[33]

Single-Color Staining

Cells were incubated with a saturating amount of primary reagent for 30 minutes at 4 C and washed twice with PBS containing 1% fetal bovine serum (FBS) and 0.1% sodium azide (PBS-azide). Cells were then stained with a saturating amount of the appropriate secondary reagent for 30 minutes at 4 C, eg, fluoresscein isothiocyanate (FITC)-goat anti-rat IgG, FITC-goat anti-mouse IgG, or FITC-avidin. After two washes with PBS-azide, samples were incubated with 1 μg/ml of propidium iodide (Sigma) just before analysis on a Cytofluorograf Model 50H with 2150 computer (Ortho Diagnostics, Westwood, MA) using an argon laser emitting at 488 nm. Particles that fluoresced red, having absorbed the propidium iodide, were considered dead and electronically excluded from the analysis.[34]

Two-Color Staining

For the simultaneous detection of L3T4 and Lyt-2, cells were exposed to the following sequence of reagents: 1) anti-L3T4 culture supernatant, 2) affinity-purified FITC-goat anti-rat IgG (H+L), 3) normal rat Ig (an $(NH_4)_2SO_4$ salt cut) plus biotinylated rat anti-Lyt-2, and 4) phycoerythrin-avidin (PE-avidin). Each incubation was for 20 minutes at 4 C followed by two washes in PBS-azide.

Monoclonal Antibodies

Anti-L3T4, clone GK 1.5,[35] and KJ16-133[36] were provided by Drs. J. Kappler and P. Marrack (National Jewish Hospital, Denver, CO). Anti-Lyt-1, clone 53.7.313,[37] anti-Lyt-2, clone 53-6.7,[37] and anti-IA^k, clone 10-2.16[38] were provided by Dr. E. Vitetta (University of Texas Southwestern Medical Center at Dallas, Dallas, TX). Anti-H-$2K^k$, clone S.17.71,[39] was provided by Dr. J. Forman (University of Texas Southwestern Medical Center at Dallas, Dallas, TX). Anti-human cytokeratin, clone BG-12,[40] which cross-reacts with mouse cytokeratin, was provided by Dr. T. Doran (Mary Kay Cosmetics, Dallas, TX). Anti-mouse β-2 microglobulin, clone 23,[41] was provided by Dr. M. Soloski (University of Texas Southwestern Medical Center at Dallas, Dallas, TX). Clones ER-TR4 and ER-TR5[15] were provided by Dr. W. van Ewijk (Erasmus University, Rotterdam, NL). Biotinylated anti-Thy1.2, clone 30-H12,[37] was purchased from Becton-Dickinson (Mountain View, CA).

Other Reagents

Rabbit anti-asialo GM_1 was purchased from Wako Chemicals, USA (Dallas, TX). FITC-PNA, FITC-avidin, and PE-avidin were purchased from Vector (Burlingame, CA), whereas FITC-goat anti-rat IgG (H+L specific), and FITC-goat anti-mouse IgG (H+L specific) were purchased from Cappel (West Chester, PA).

Preparation of Frozen Sections

Fresh tissue was frozen in 2-methylbutane at −70 C and embedded in OCT compound for sectioning. Six-micron sections were fixed for 5 minutes in ice-cold acetone.

Histochemical Techniques

Nonspecific esterase staining was performed according to the method of Yam et al[42]; acid phosphatase staining was performed according to the method of Barka et al.[43]

Immunoperoxidase Method

Sections were incubated overnight with primary antibody diluted 1:10 in PBS and then washed three times for 5-minute intervals in cold PBS. Next, sections were incubated for 90 minutes with peroxidase-conjugated secondary antibody diluted 1:10 in PBS. After three more washes in cold PBS, sections were developed for 15 minutes in the Hanker-Yates substrate[44] dissolved in PBS.

Tdt Staining

Cytocentrifuge preparations were stained for terminal deoxyribonucleotidyl transferase (Tdt) using a Tdt-immunofluorescence kit (Supertechs, Inc., Bethesda, MD) that was the gift of Dr. Fred Bollum.

Electron Microscopy

Tissues were fixed in 2.5% glutaraldehyde and 1% formaldehyde in 0.1 M sodium cacodylate buffer, pH 7.4, for 2 hours; postfixed for 1 hour in 2% osmium tetroxide in the buffer; dehydrated in graded acetone-water; and embedded in 27.3% Araldite epoxy resin 502, 18.8% Polybed 812, 52.8% dodecenylsuccinic anhydride, and 1.1% DMP-30 (Polysciences, Warrington, PA). Sections stained with 5% uranyl acetate and Reynold's lead citrate were examined with a JEOL JEM 100B electron microscope.

Cell Culture and Limiting-Dilution Analysis

The frequency of cell proliferation in response to Con A, IL-2-containing supernatant, and splenic accessory cells (SAC) was determined using limiting-dilution analysis with linear regression statistical analysis. The complete culture medium used and the method for generation of irradiated SAC cultures have been described previously.[45] Briefly, variable numbers of fresh thymocytes, lymphocytes from tumors, or spleen cells were added in 10 μl per SAC-containing well of medium supplemented with 2 μg/ml Con A and 50% IL-2-containing supernatant. (IL-2-containing medium was prepared by culturing 5×10^6 C3H/Bi spleen cells in complete culture media supplemented with 2 μg/ml Con A at 37 C and harvesting the supernatant after 24 hours.) Wells were scored positive or negative for proliferation after 7 days of culture by visual inspection using a Leitz inverted phase microscope. Tissue explants were cultured in 60-mm Petri dishes (Falcon) with complete culture medium in a 37 C incubator with 5% CO_2.

Table 1. *Tumor Incidence at Necropsy for C3H/Bl Mice Injected with PTA-5 as Neonates*

Tumors	Total animals with tumors	Incidence from birth (N = 303)	Incidence from 3 weeks (N = 230)
Thymic	140	46.2%	60.9%
Hair follicle	78	25.7%	33.9%
Mammary gland	35	11.6%	15.2%
Salivary gland	60	19.8%	26.1%
Miscellaneous (thyroid, prostate, renal)	4	1.3%	1.7%
Total	205	67.7%	89.1%

Results

Necropsy Data: Neonatal Infection With Py Induces Thymic Tumors

As shown in Table 1, 67.7% of the C3H/Bittner mice injected with PTA-5 developed tumors. Four tumor types were seen commonly: thymic tumors, hair follicle tumors, mammary gland tumors, and salivary gland tumors. Two or more of these tumor types were observed often in individual animals (data not shown).

The presence of thymic tumors could be detected 1 to 2 weeks before death because the affected animals developed breathing difficulty as the tumors displaced other thoracic organs. In Figure 1, the gross necropsy of an animal with a typical thymic tumor is contrasted to a normal necropsy. An average thymic tumor weighed ten times more than a normal thymus (Table 2). These tumors commonly contained more lymphocytes than age-matched control thymuses, although due to the larger mass of tumors the tumors were lymphopenic relative to normal thymuses (Table 3).

Histology of Py-Induced Thymic Epithelial Tumors

The tumors are similar in histologic appearance to human spindle cell thymomas.[28] In Figure 2, the microscopic appearance of a C3H/Bittner thymic tumor, with large homogeneous areas of epithelium interspersed with islands of lymphocytes, is shown. Mitotic figures are evident among the epithelial cells. Although the microscopic appearance suggested a high grade of neoplasia, these tumors were never metastatic, and rapid death of the animals was due to local compressive effects of the tumors. The epithelial cells had larger, less basophilic nuclei than lymphocytes. Keratin pearls, frequently present in squamous carcinomas, and Hassal's corpuscles, present in normal thymic medulla, were not evident in these tumors. In very large

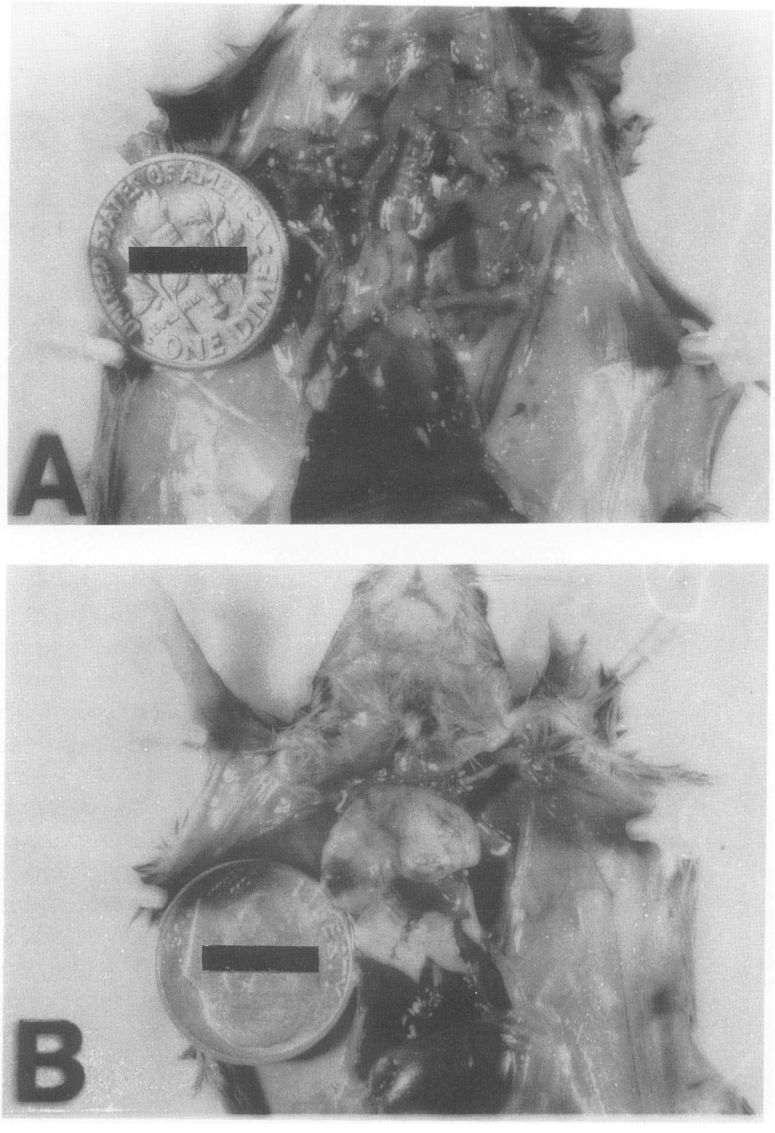

Figure 1. **A:** *A necropsy of a normal 6-week-old C3H/Bi is shown for comparison. The thymus weighed 48.5 mg.* **B:** *A necropsy of a 6-week-old C3H/Bittner injected with polyoma virus 1 day after birth; when killed, this animal was showing signs of severe dyspnea. The thymic tumor weighed 535 mg. In many of the tumor-bearing animals, such as this example, both lobes of the thymus were enlarged by tumor. All of the thymic tumors necropsied were encapsulated without extension to adjacent viscera.*

thymic epithelial tumors, areas of infarction and dystrophic calcification were identified. The thymic capsule was thickened, from one- or two-cell layers surrounding normal thymus, to six- to eight-cell layers. The tumors frequently invaded beyond the margin of the residual thymic capsule, yet did not adhere to nearby organs.

In Figure 3, the ultrastructural appearance of a thymic epithelial tumor is shown. It was essentially identical to that of normal thymic epithelium with little evidence for a secretory function because of a paucity of organelles and rough endoplasmic reticulum. Tonofilaments and desmosomes confirmed the epithelial nature of these tumors.

Table 2. *Thymic Tumor Statistics*

Thymic tumor mass (mg), 643 ± 275* (N = 78)
Normal thymus mass (mg), 55 ± 9.7* (N = 19)
Age at necropsy, 87 ± 40 days* (range, 36 to 219 days)
Lymphocytes/tumor, 1.02 ± 0.3 × 10^8 cells* (N = 17)
Lymphocytes/normal thymus, 3.3 ± 1.4 × 10^7 cells* (N = 12)

* Mean ± SD.

Immunohistologic and histochemical techniques were employed to examine how stromal organization was altered in the tumors compared with normal thymus and involuted thymus of steroid-treated mice (Figure 4). In cortisone-induced thymic involution, because the cortex is almost completely depleted of lymphocytes, stromal organization appears more obvious due to the condensation of cortical stromal elements.

An anticytokeratin MAb was used to demonstrate the distribution of all epithelial cells. In normal thymus (Figure 4A), the cortical epithelial cells showed a diffuse dendritic distribution, whereas the medullary epithelial cells appeared as condensed areas.[46] The tumor was dominated by areas of solid tumor epithelium (TE) interspersed with

Table 3. *Cellularity of Thymic Tumors*

Tumor	Sex	Age (days)	Organ mass (mg)	Lymphocytes ($\times 10^7$)	Cellularity index*
Normal thymuses (N = 17)	M	42–56 (range)	56.2 ± 4.7†	3.98 ± 0.80†	7.10 ± 1.44†
Individual thymic tumors					
	M	73	1,038	2.72	0.26
	M	53	747	2.60	0.35
	F	83	538	2.47	0.46
	M	99	726	3.81	0.52
	M	82	612	3.32	0.54
	M	68	477	2.89	0.60
	F	65	595	3.99	0.67
	M	45	700	5.52	0.79
	M	79	773	6.17	0.80
	M	47	210	2.10	1.00
	M	73	584	6.73	1.15
	F	56	837	17.60	2.10
	M	47	585	15.10	2.58
	F	79	798	25.50	3.20
	F	88	170	8.96	5.27
	F	62	580	34.10	5.88
	M	62	414	31.30	7.56

* Cellularity index, lymphocytes/organ mass (cells $\times 10^5$/mg tissue).
† Mean ± SD.

infrequent islands of lymphocytes (LY) supported by a dendritic epithelial network (Figure 4B).

Normal thymus stained with anti-IA^k (Figure 4C) showed the same staining pattern as the anti-cytokeratin MAb, because practically all thymic epithelial cells are Ia^+.[47] With hydrocortisone treatment (Figure 4D), the loss of cortical thymocytes caused the cortical epithelium to compact into a confluent Ia^+ zone; the epithelium-rich me-

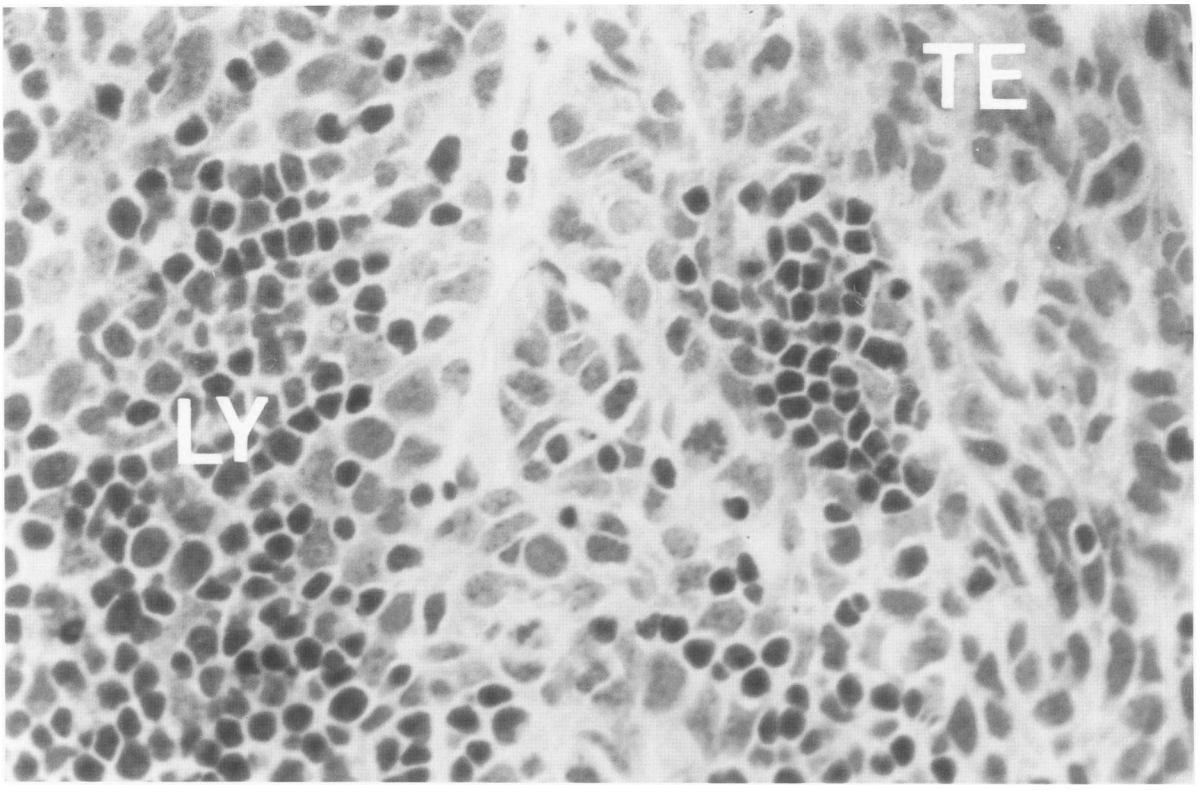

Figure 2. *H&E-stained paraffin section of polyoma virus-induced thymic epithelial tumor. Large areas are composed of polygonal epithelial cells without lymphocytes. This section illustrates two islands of lymphocytes surrounded by tumor epithelium. Several epithelial mitotic figures are seen in this photograph. TE, a region of tumor epithelium; LY, an island of lymphocytes.*

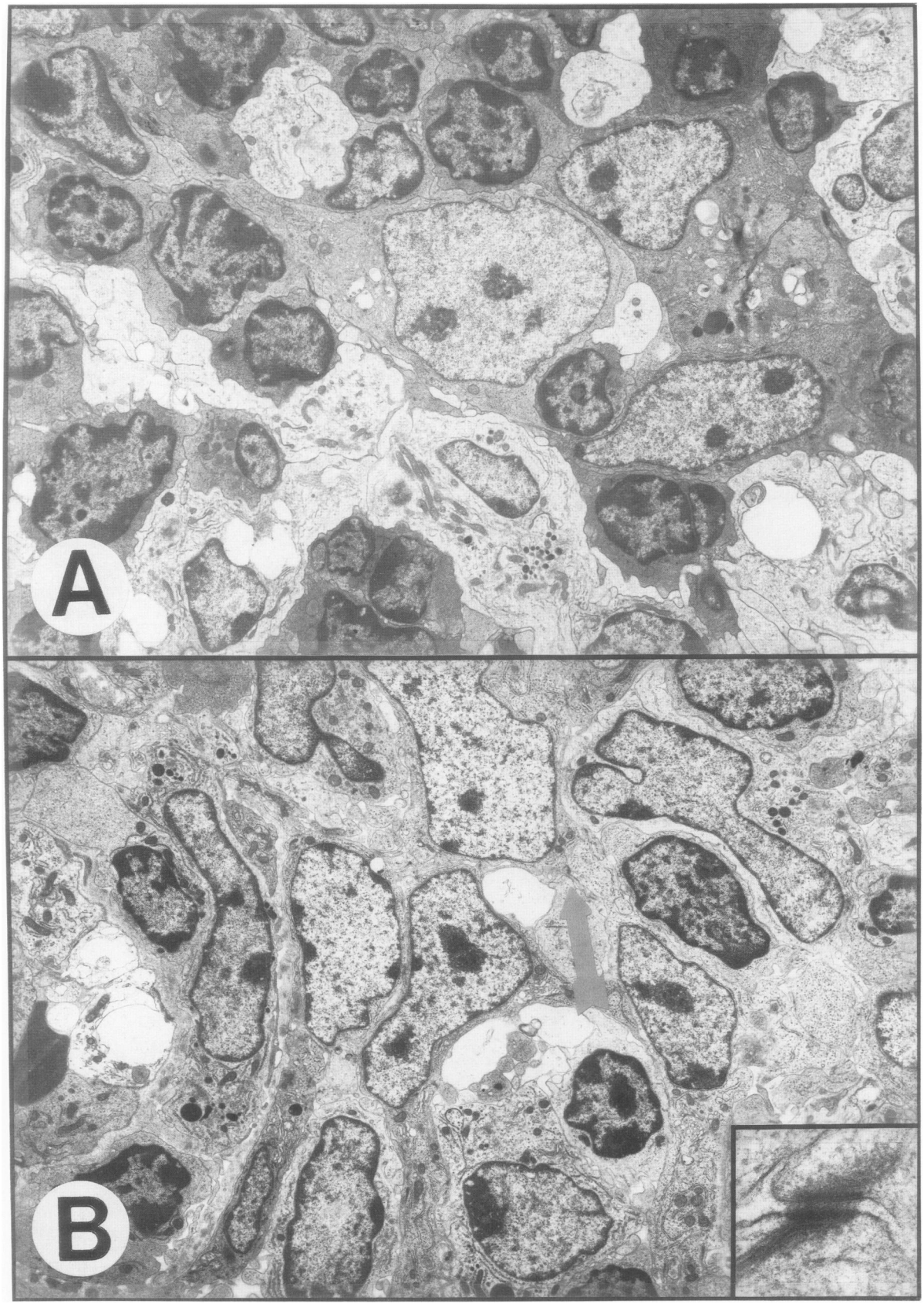
A
B

Figure 3. *An electron micrograph of normal medullary thymic epithelium* **(A)** *and tumor epithelial cells* **(B).** *There are no ultrastructural differences between thymic tumor epithelium and normal thymic epithelium. The cell nuclei are large and oval to fusiform in shape. Cytoplasmic organelles are lacking. The scarcity of rough endoplasmic reticulum, vacuoles, and Golgi suggests that extracellular secretion is not a significant activity of these cells. Several desmosomes are present in the photo but are difficult to discern at this magnification. Arrows point to desmosomes (A and B, original magnification ×4000).* **Inset:** *A desmosome intercellular bridge with radiating tonofilaments is seen in this electron micrograph of tumor epithelium. The presence of desmosomes and tonofilaments, which were also detected by cytokeratin immunoperoxidase staining, confirms the epithelial nature of these tumors (original magnification ×90,000).*

dulla was also Ia$^+$. Clusters of intensely Ia$^+$ cells in the medulla close to the cortico-medullary (c-m) junction in involuted thymus corresponded to the nonspecific esterase-positive population of IDCs (vide infra). Tumor sections stained with anti-IA^k (Figure 4E) showed a staining pattern similar to anti-cytokeratin (Figure 4B).

An anti-β_2-microglobulin (β_2M) MAb, detecting all Class I MHC antigens, stained normal medullary epithelium intensely but cortical epithelium weakly (Figure 4F). However, cortical blood vessels were prominently highlighted. Anti-β_2M reacted with all epithelial elements of steroid-involuted thymus (Figure 4G). Within the tumors, solid areas of neoplastic epithelium stained homogeneously with anti-β_2M, whereas only blood vessels were stained within lymphocyte-rich regions (Figure 4H).

We showed[48] that an anti-asialo-GM$_1$ antiserum reacts with all murine thymic epithelial cells in the medulla and a substantial number of the Ia$^+$ epithelial cells in the cortex (Figure 4I). In serial sections, tumor epithelium that appeared homogeneous when stained with hematoxylin and eosin (H&E) was revealed with anti-asialo-GM$_1$ to have heterogeneity, with areas of heavy staining, areas of stippled staining, and areas of no staining (Figure 4J). This same heterogeneity was revealed using two MAbs that differentiate between thymic cortical and medullary epithelium. ER-TR4-stained normal cortical epithelium (Figure 4K), whereas ER-TR5 stained normal medullary epithelium (Figure 4N) on normal thymus.[15] The staining distribution of these two reagents was more discrete on sections of mouse thymus after hydrocortisone-induced involution because of epithelial condensation with loss of lymphocytes (Figure 4L, O). Thymic tumors stained with ER-TR4 and ER-TR5 showed heterogeneous reactivity similar to anti-asialo GM$_1$ reactivity on these tumors (Figure 4M, P). Within islands of lymphocytes, the epithelium was ER-TR4$^+$, ER-TR5$^-$ (not shown), ie, identical in phenotype with normal cortical epithelium. After examining many thymic epithelial tumors, our impression was that these lymphocyte-rich islands, which often abutted the tumor capsule, represented normal cortical thymic tissue pushed to the periphery of the tumor with its expansion.

Two nonepithelial stromal cell types believed to play a role in T cell maturation are thymic macrophages and IDCs.[49–53] Murine thymic macrophages were localized by staining for acid phosphatase, an enzyme present in lysosomes. In the normal thymus, macrophages with intense acid phosphatase activity were scattered throughout the cortex with accumulation along the cortical side of the c-m junction, whereas IDCs in the medulla stained weakly for acid phosphatase (Figure 4Q). The cortical distribution of thymic macrophages was retained with steroid-induced involution (Figure 4R). Macrophages in the tumors were localized to the islands of residual normal thymic cortex (Figure 4S). Weak acid phosphatase activity was present, however, throughout the tumors, being present in the neoplastic epithelial cells.

Conversely, intense staining for nonspecific esterase in the normal murine thymus was localized to IDCs, which were exclusive to the thymic medulla, whereas weak nonspecific esterase staining identifies cortical thymic macrophages (Figure 4T). In steroid-involuted thymus, nonspecific esterase activity remained localized in the medulla, typically along the medullary side of the c-m junction (Figure 4U). Comparisons of serial sections from involuted thymus stained with anti-IA^k and nonspecific esterase indicated that IDCs are responsible for the pattern of very intense IA^k-staining along the medullary side of the c-m junction. Only one tissue block examined from seven tumors was found to have a lymphoid island containing intensely nonspecific esterase positive IDCs identifying an island of normal thymic medulla (Figures 4 and 5). The rarity of such normal medullary islands suggested that normal thymic medulla was commonly distorted or obliterated by the expanding intrathymic tumor mass, whereas normal cortical islands were pushed outward by the tumor but remained intact. Weak nonspecific esterase activity was found uniformly in the tumor epithelial cells.

Lymphocytes within the tissues were visualized with an anti-Lyt-2 mAb. Lyt-2, which is expressed on most cortical thymocytes,[54] displayed a homogeneous lymphoid staining pattern in normal thymic cortex. Because only one of three medullary lymphocytes are Lyt-2$^+$, the normal thymic medulla had a stippled appearance (Figure 4W). With hydrocortisone-induced thymic involution, the normal medullary stippled pattern of Lyt-2 staining was retained; however, the cortex was depleted of all Lyt-2$^+$ lymphocytes (Figure 4X). In thymic epithelial tumors, islands of normal cortical lymphocytes also stained uniformly with anti-Lyt-2 (Figure 4Y). Additionally, anti-Lyt-2 staining revealed that areas of tumor epithelium (TE) contained a sparse population of lymphocytes.

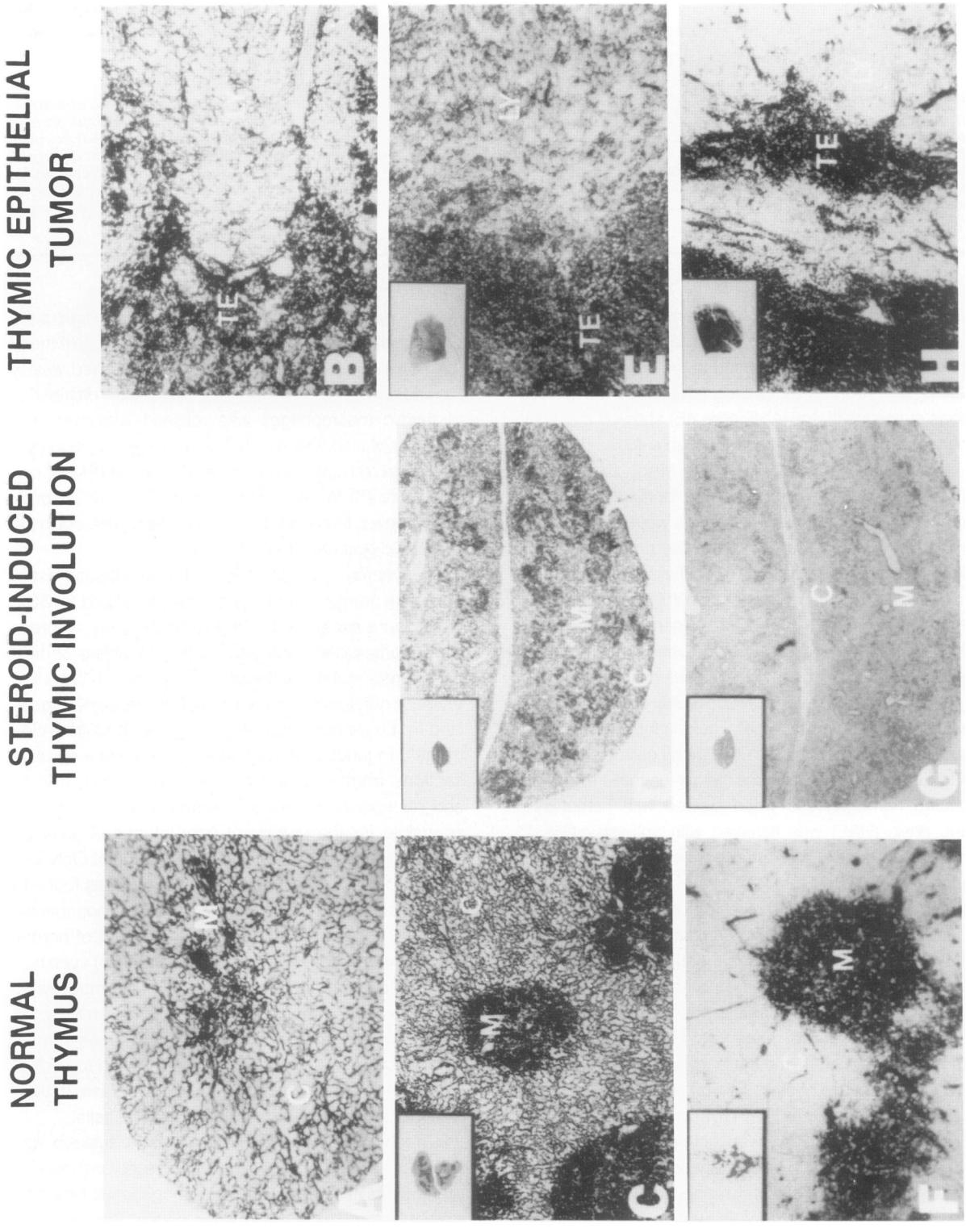

Figure 4. *These photographs represent frozen sections stained by immunoperoxidase and histochemical techniques. The panels on the left side (normal thymus) are examples of thymus from normal 6-week-old C3H/Bittner mice; the middle column (steroid-induced thymic involution) shows thymus harvested 3 days after bolus injection of 4 mg intraperitoneally of hydrocortisone; and the panels on the right (thymic epithelial tumor) are thymic epithelial tumors generated by injection of neonates with polyoma virus. C, thymic cortex; M, thymic medulla; TE, tumor epithelium; LY, island of cortical lymphocytes in tumor. Insets are low-magnified views of the entire tissue sections for orientation.* **A** *and* **B**: *Anti-cytokeratin.* **A**: *Cytokeratin staining of normal thymus shows a dendritic epithelial pattern in the cortex and an isolated region of denser medullary staining.* **B**: *An area of solid tumor epithelium (left side of photo) stains densely with anti-cytokeratin, whereas a lymphocyte-rich region (right side of photo) shows dendritic staining like normal thymic cortex.* **C, D,** *and* **E**: *Anti-Ia^k.* **C**: *IA^k expression of normal thymic cortex is demonstrated by dendritic staining, whereas medullary areas show partially confluent staining, similar to staining with anti-cytokeratin.* **D**: *IA^k staining of steroid-involuted thymus shows a confluent staining of cortex due to loss of lymphocytes; medulla also stains confluently with IDCs at the c-m junction staining very intensely.* **E**: *An area of solid tumor epithelium (left side of photo) stains intensely with IA^k, whereas a lymphoid island (right side of photo) shows dendritic staining like normal cortex.* **F, G,** *and* **H**: *Anti-β_2M.* **F**: *In normal thymus, anti-β_2M stains cortical blood vessels intensely, but only weakly stains the cortical epithelial network, whereas it stains the medulla with a partially confluent pattern.* **G**: *Anti-β_2M stains steroid-involuted thymus in a confluent manner (both cortex and medulla) with IDCs staining intensely at the c-m junction.* **H**: *Anti-β_2M stains solid areas of tumor epithelium intensely, whereas only blood vessels show staining in lymphocyte-rich areas.*

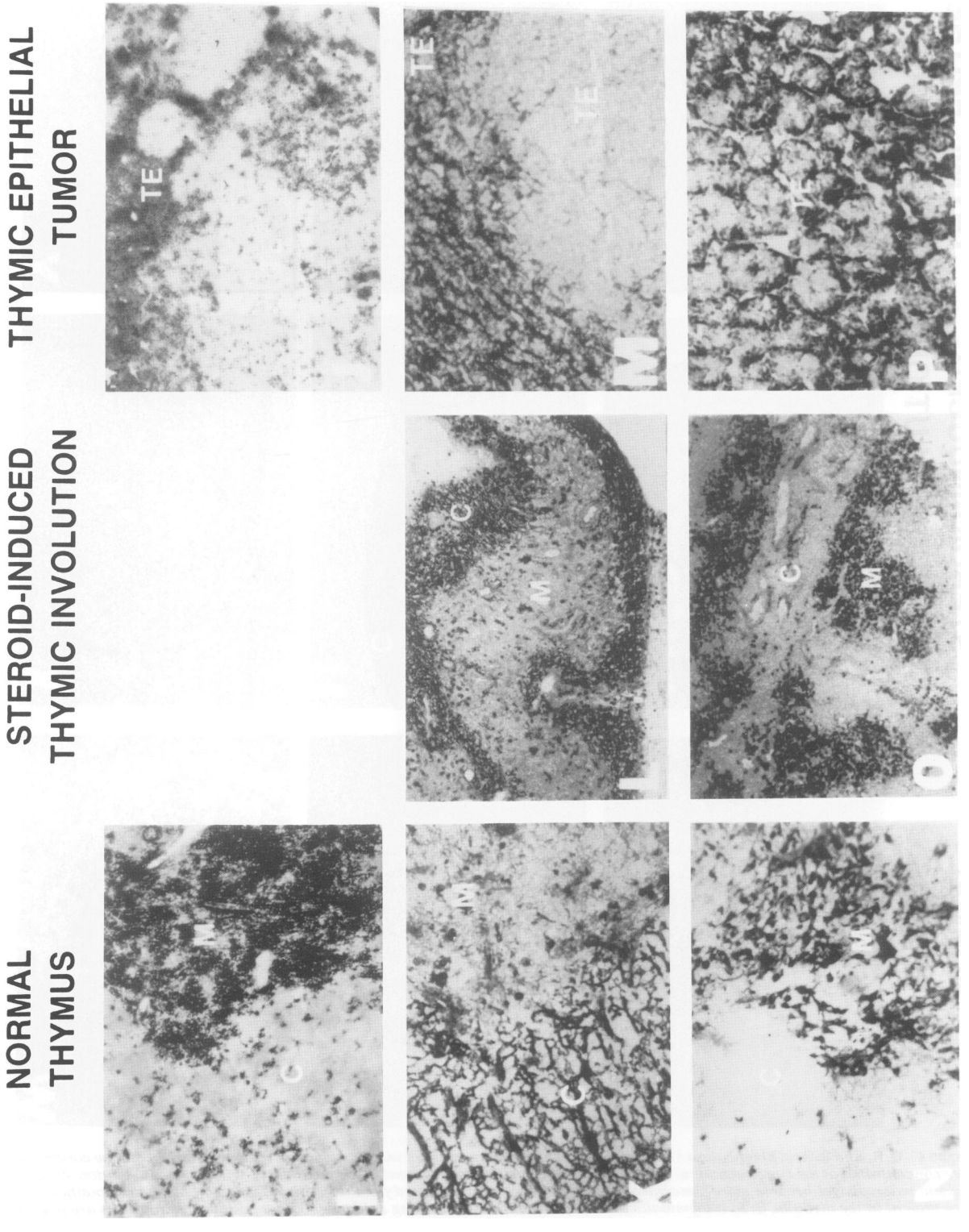

Figure 4. **I, J:** *Anti-asialo-GM_1.* **I:** *Anti-asialo-GM_1 stains scattered normal cortical epithelial cells (left side of photo) and stains medulla semiconfluently (right side of photo).* **J:** *Anti-asialo-GM_1 stains continuous areas of tumor epithelium (which is the entire photo) in heterogeneous fashion.* **K, L,** *and* **M:** *ER-TR4.* **K:** *ER-TR4 stains the normal cortical dendritic epithelial network intensely (left side of photo) while only staining a small subset of medullary cells.* **L:** *With steroid involution, ER-TR4 stains the condensed cortical rim of epithelium intensely in confluent fashion while staining a small subset of medullary epithelium.* **M:** *ER-TR4 stains solid areas of tumor epithelium (the entire photo) in a heterogeneous fashion.* **N, O,** *and* **P:** *ER-TR5.* **N:** *Only a few cortical epithelial cells stain with ER-TR5 (left side of photo) in normal thymus, whereas a large number of medullary epithelial cells stain intensely (right side of photo).* **O:** *With steroid involution. ER-TR5 continues to stain medullary areas intensely but only stains scattered cortical epithelial cells, despite the cortical epithelium being condensed by involution.* **P:** *ER-TR5 shows heterogeneous staining on solid tumor epithelium (the entire photo).*

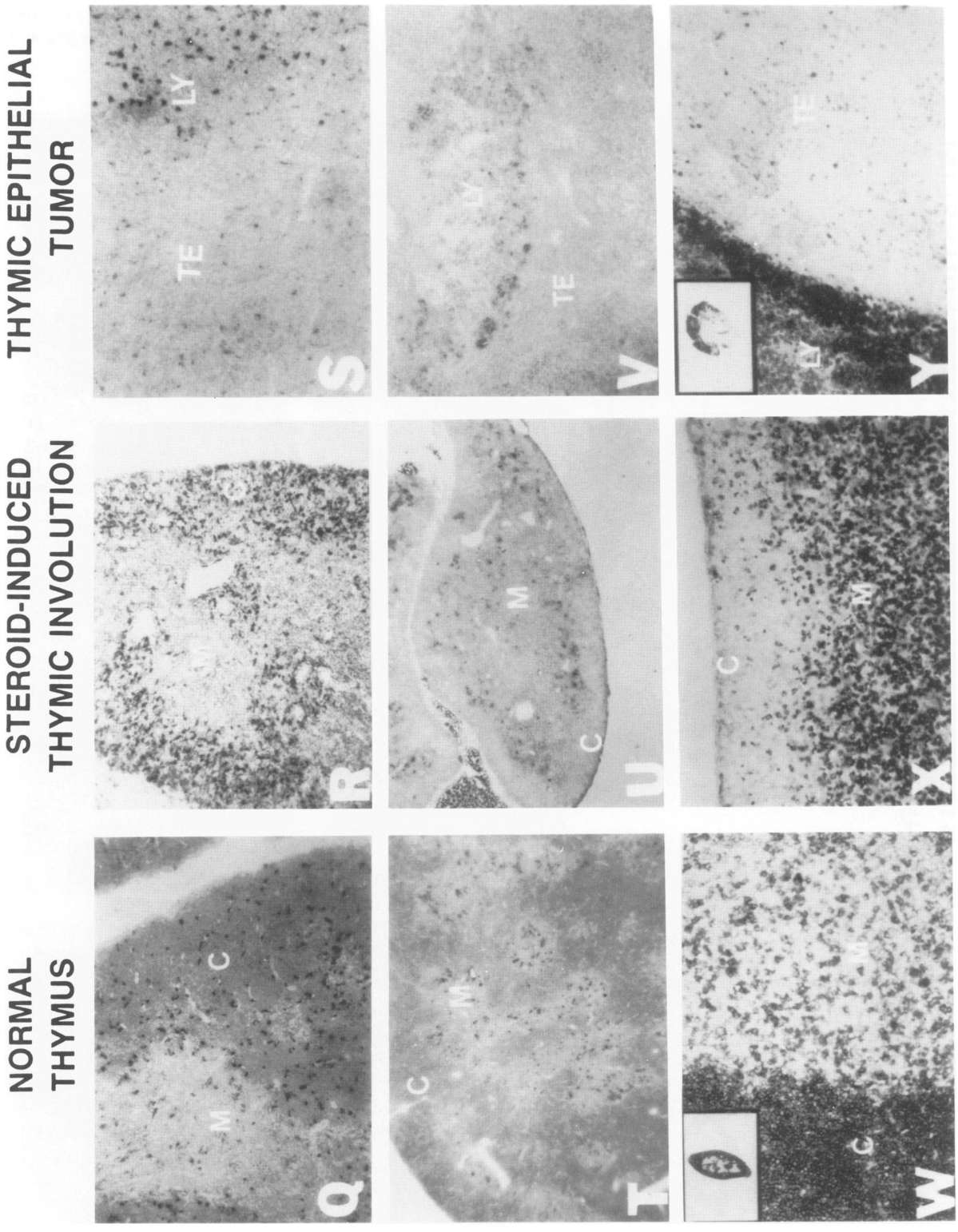

Figure 4. **Q, R,** *and* **S:** *Acid phosphatase.* **Q:** *Intensely acid phosphatase-stained macrophages are scattered throughout the cortex, but are concentrated at the c-m junction, whereas weaker staining IDCs are present in the medulla.* **R:** *With steroid involution, cortical thymic macrophages become more concentrated as lymphocytes are depleted from the cortex; few acid phosphatase-positive cells are present in the medulla.* **S:** *In a thymic tumor, numerous intensely staining acid phosphatase-positive macrophages are present in a lymphoid island (right side of photo), whereas they are more scattered in epithelial areas (left side of photo).* **T, U,** *and* **V:** *Nonspecific esterase.* **T:** *Esterase-positive IDCs are present only in the thymic medulla.* **U:** *With steroid involution, esterase-positive IDCs remain on the medullary side of the c-m zone.* **V:** *A rare island of medulla with lymphocytes and esterase-positive IDCs is seen within a thymic tumor (top of photo).* **W, X,** *and* **Y:** *Anti-Lyt-2.* **W:** *Anti-Lyt-2 stains nearly all cortical thymocytes (left side of photo) in normal thymus, whereas only scattered Lyt-2-positive cells are present in the medulla (right side of photo).* **X:** *With steroid involution, the cortex (top of photo) is almost entirely depleted of Lyt-2-positive lymphocytes, whereas numerous Lyt-2-positive lymphocytes are present in the medulla (bottom of photo).* **Y:** *Cortical islands rich in lymphocytes stain homogeneously with anti-Lyt-2 (left side of photo), whereas, in areas of solid tumor epithelium, only scattered lymphocytes are stained (right side of photo).*

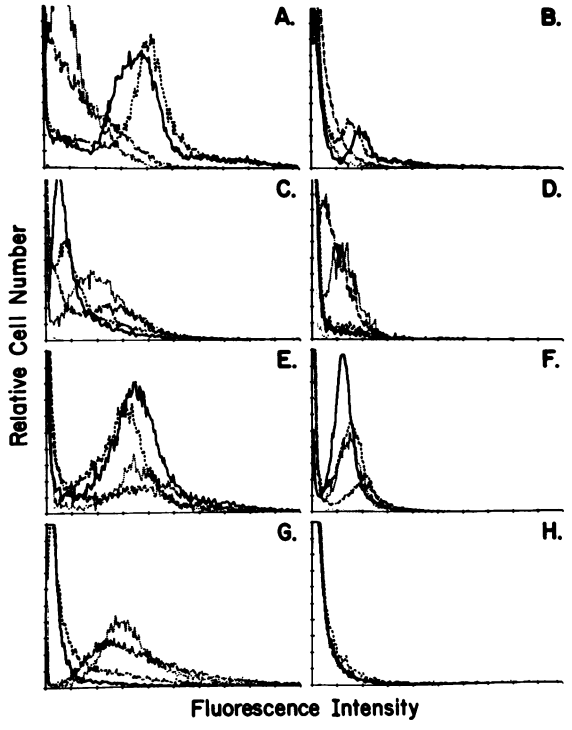

Figure 5. *Fluorescence intensity profiles for a panel of murine T cell epitopes compare lymphocyte suspensions obtained from normal thymus (——), a thymic epithelial tumor (- - -), hydrocortisone-induced involution of normal thymus (·····), and hydrocortisone-induced involution of a thymic epithelial tumor (-·-·-·).* **A:** *Anti-Thy1.2.* **B:** *Peanut agglutinin (PNA).* **C:** *Anti-Lyt-1.* **D:** *KJ16-133.* **E:** *Anti-Lyt-2.* **F:** *Anti-L3T4.* **G:** *Anti-H-2K^k.* **H:** *Anti-IA^k.*

Phenotype of Lymphocytes in Thymic Epithelial Tumors

Cortical thymocytes, which represent 70% of all thymocytes, have a unique phenotype that discriminates them from medullary thymocytes, cortisone-resistant thymocytes (CRTs) and resting peripheral T cells. Cortical thymocytes are Thy1.2^{bright}, Lyt-1^{dim}, MHC Class I^{dim}, PNA$^+$, J11d$^+$, mostly ThB$^+$, Tdt$^+$, and coexpress L3T4 and Lyt-2. In contrast, the three more mature cell populations are Thy1.2^{moderate}, Lyt-1^{bright}, MHC Class I^{bright}, PNA$^-$, J11d$^-$, ThB$^-$, Tdt$^-$, and are either Lyt-2$^+$L3T4$^-$ or Lyt-2$^-$L3T4$^+$.[54-58]

Histologic studies suggested that the tumors contained regions of preserved thymic cortex with distortion or obliteration of medullary architecture by tumor growth. We studied the phenotype of the lymphocytes within the tumors to determine if the neoplastic epithelium had an effect on lymphocyte development.

Lymphocytes obtained from three thymic tumors were compared with lymphocytes from normal thymus for intracytoplasmic staining with anti-Tdt.[59] More than 80% of the lymphocytes from the tumors were Tdt$^+$, a characteristic of cortical thymocytes (data not shown).

Flow cytometric analysis of tumor-derived lymphocytes identified a cell surface phenotype typical of cortical thymocytes (Table 4). Significant fractions of cells from tumor T30 were PNA$^+$, J11d$^+$, and ThB$^+$. Moreover, the high frequencies of the L3T4$^+$ and Lyt-2$^+$ cells in the tumors T30, T25, and T26 suggested the presence of an L3T4$^+$Lyt-2$^+$ population (vide infra).

Fluorescence intensity profile comparisons were made between lymphocytes in the thymic epithelial tumors, normal thymocytes (predominantly immature cortical thymocytes), and CRTs. Most lymphocytes from both a thymic tumor and a normal thymus were Thy1.2^{bright}, Lyt-1^{dull}, H-2K$^{k\ dull}$, and PNA$^+$ (Figure 5). Of normal thymocytes, 2% to 3% in the C3H/Bittner strain and 2% to 3% of tumor lymphocytes stained with KJ16-133 MAb, which recognizes a subset of T cell receptors. In comparison, cortisone-resistant thymocytes were Thy1.2^{dull}, Lyt-1^{bright}, H-2K$^{k\ bright}$, and PNA$^-$; and 20% of the CRTs were KJ16-133$^+$.

Demonstration of Double-Positive Lymphocytes in the Tumors

Two-color analysis for the simultaneous detection of the Lyt-2 and L3T4 markers indicated that the tumor lymphocyte population contained a large subset of double-positive L3T4$^+$Lyt-2$^+$ cells (Figure 6), as suggested by the overlap of L3T4$^+$ cells and Lyt-2$^+$ cells detected in single-color analysis. The presence of L3T4$^+$Lyt-2$^-$ and L3T4$^-$Lyt-2$^+$ subsets suggested that a medullary thymic compartment was also present in the tumors. Four of five tumors reported in Table 5 had a smaller fraction of double-positive cells and larger fractions of single-positive cells than normal thymus. The ratio of L3T4$^+$Lyt-2$^-$ to L3T4$^-$Lyt-2$^+$ cells was lower in these four tumors than the ratio in normal thymus. This data showed that the medullary thymocyte compartment was enlarged compared with the cortical compartment in most of the tumors. An actual expansion of the medullary microenvironment by the neoplastic process might have occurred.

Steroid Responsiveness

An animal with a thymic tumor was injected with a bolus of hydrocortisone three days before it was killed. The fluorescence intensity profiles of cortisone-resistant lymphocytes from this tumor were identical to those of CRTs obtained from a normal animal treated similarly (Figure 5).

Table 4. *The Cell Surface Phenotype of Lymphocytes Obtained from Thymic Epithelial Tumors*

Surface marker	Normal thymus*	Lymphocytes from individual thymic tumors (%)						
		T30	T25	T26	T12	T14	T16	T17
Thy 1.2	97	88	97	92	91	93	88	95
Lyt-1	92	91	94	95	91	92	87	93
Lyt-2	89	78	85	69	88	82	78	82
L3T4	90	74	93	71	ND	ND	ND	ND
PNA	84	63	92	93	71	94	70	63
J11d	86	66	ND	ND	ND	ND	ND	ND
ThB	65	49	ND	ND	ND	ND	ND	ND
H-2K^k	76	88	67	79	90	85	84	80
IA^k	28	ND	47	40	57	35	34	33

* Thymocyte cell suspension obtained from normal 6-week-old C3H/Bi thymus. An average from two experiments is reported.
ND not done.

Frequency of Functionally Mature Lymphocytes in the Tumors

Because there was a greater proportion of single-positives, ie, Lyt-2$^+$L3T4$^-$ and Lyt-2$^-$L3T4$^+$ cells, to double-positives, ie, Lyt-2$^+$ L3T4$^+$ cells, we reasoned that there might have been a higher frequency of lymphocytes capable of proliferating in response to Con A plus IL-2-containing supernatants in the tumors than in normal thymus. In Table 6, the frequency of proliferating lymphocytes from two thymic tumors was less than the frequency in normal spleen but was significantly higher than the frequency in normal thymus. Both of these tumors had a higher fraction of single-positive lymphocytes than did the normal thymus. The frequency of proliferating cells in a third tumor was similar to that occurring in the normal thymus, consistent with the low fraction of single-positive cells in this tumor.

Establishment of Thymic Tumor Explants In Vitro

Thymic tumor fragments formed adherent explants with epithelial characteristics after two to three weeks in primary culture (Figure 7). Tonofilaments and desmosomes were identified by electron microscopy (data not shown).

Discussion

Thymic epithelium plays a significant role in the intrathymic development of T lymphocytes, although a precise understanding of the events is lacking. One avenue for the study of normal thymic epithelium function has been the study of thymomas, ie, thymic epithelial tumors.

Human thymic epithelial tumors can be associated with other diseases, in particular, myasthenia gravis, pure red blood cell aplasia, acquired hypogammaglobulinemia, and a variety of autoimmune diseases.[60] These human thymic epithelial tumors display considerable histologic variation in both epithelial morphology and in the ratio of the epithelial tumor component to the normal lymphocyte component.[28,61] In general, human thymic epithelial tumor-associated lymphocytes are phenotypically similar to normal cortical thymocytes ie, T4$^+$T8$^+$, T6$^+$, T11$^+$, Tdt$^+$, T3$^-$, PNA$^+$,[25,62] although there was one report of a human thymic epithelial tumor infiltrated predominantly with large immature prothymocytes.[26] Phenotypic variation in the ratio of cortical thymocytes to medullary thymocytes appears to be correlated with the functional ability of the tumor-associated lymphocytes to respond to PHA by proliferation in culture. Tumors with a greater percentage of T3$^+$T6$^-$PNA$^-$ medullary-type thymocytes respond better to mitogen in culture than do tumors with a larger fraction of T3$^-$T6$^+$PNA$^+$ cortical-type lympho-

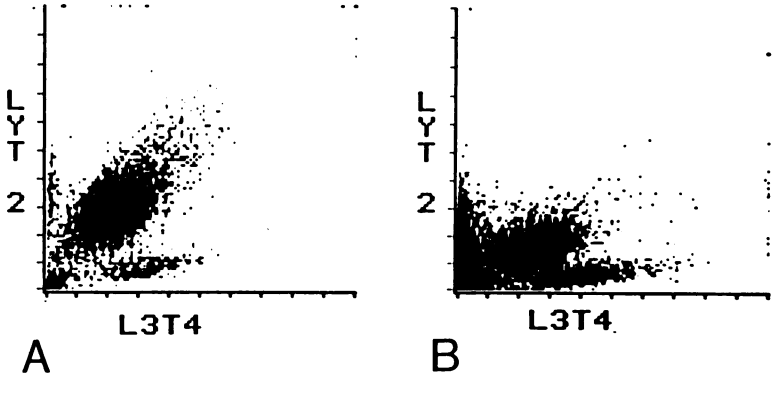

Figure 6. *Two color fluorescence cytograms for* (A) *lymphocytes from normal thymus and* (B) *lymphocytes from a thymic epithelial tumor. Lyt-2-staining fluorescence (red) is on the Y-axis, whereas L3T4 staining fluorescence (green) is on the X-axis.*

Table 5. *Two Color Flow Cytometric Analysis of LYT-2 and L3T4*

Sources of lymphocytes	$L3T4^+Lyt\text{-}2^+$ (%) (double positive)	$L3T4^-Lyt\text{-}2^+$ (%) (Lyt-2 only)	$L3T4^+Lyt\text{-}2^-$ (%) (L3T4 only)	Ratio of ($L3T4^+$ only/ $Lyt\text{-}2^+$ only)	Ratio of double positive/Single
Normal thymus 1	81.9	2.8	7.2	2.57	8.19
Normal thymus 2	75.1	3.0	14.5	4.83	4.29
Normal thymus 3	72.5	3.1	8.1	2.61	6.47
Mean normal values (mean ± SD)	76.5 ± 4.9	3.0 ± 0.2	9.9 ± 3.9	3.34 ± 1.29	6.32 ± 1.95
Tumor 1	50.5	16.6	13.5	0.81	1.68
Tumor 2	45.1	15.2	19.5	1.28	1.30
Tumor 3	56.2	10.7	14.8	1.38	2.20
Tumor 4	44.5	11.6	19.8	1.71	1.42
Tumor 5	50.6	9.1	23.9	2.63	1.53
Tumor 6*	78.9	3.5	8.9	2.54	6.36
Mean tumor values (mean ± SD)	54.0 ± 12.8	11.2 ± 4.7	16.7 ± 5.4	1.73 ± 0.73	1.42 ± 2.0

* The values for tumor #6 were similar to those values from normal thymus.

cytes.[63] Histologic studies of the epithelial component of human thymic epithelial tumors showed that the neoplastic epithelial cells are $HLA\text{-}DR^+$, $cytokeratin^+$, and $A_2B_5{}^+$ similar to normal human thymic epithelium.[25] Chilosi et al[61] described a tumor with both normal cortical and medullary lymphocytes surrounded by neoplastic medullary epithelium identified by a medullary epithelium-specific marker, RFD-4.

Complementary to studies of spontaneous human thymomas, there have been efforts to deliberately generate experimental murine thymic epithelial tumors. Stutman and colleagues injected neonatal mice intrathymically with 7,12-dimethylbenz(a)anthracene resulting in a very low frequency of carcinogen-induced thymic epithelial tumor development.[20-23] One tumor was shown on serial transplantation to reconstitute skin graft rejection responses and graft *versus* host responses and to improve survival rates in neonatally thymectomized, syngeneic recipients. The tumor slowly lost the ability to restore immune function after multiple animal passages; however, two phenotypically distinct tumor sublines were derived by partial subcloning *in vivo*. Neither subline alone was able to reconstitute immune functions in neonatally thymectomized animals, but deliberately mixed sublines were able to restore immune functions in a manner similar to the original parent tumor. Stutman et al assumed that the "round" cell type arose from transformed thymic epithelial cells, whereas the "spindle" cell type arose from transformed mesenchymal cells. With hindsight, we speculated that the "spindle" cell type actually arose from a second thymic epithelial subset, a logical assumption because spindle cell thymomas in humans are epithelial in origin despite their mesenchymal appearance. Unfortunately, monoclonal antibodies for detecting lymphocyte differentiation antigens and thymic cortical and medullary epithelial subset markers (eg, ER-TR4 and ER-TR5) were not available at the time of Stutman's pioneering work.

Using Py virus rather than a chemical carcinogen to induce tumors, Law et al[64] published evidence that neonatally thymectomized mice could be restored immunologically by subcutaneous implants of fragments from primary thymic epithelial tumors that developed in C3H/LW

Table 6. *The Frequency of Lymphocytes from Thymic Epithelial Tumors Capable of Responding by Proliferating in Response to CON A and IL-2 Supernatants*

Lymphocyte source	Frequency of cells proliferating under microculture conditions*	$Lyt\text{-}2^+L3T4^+$ (%)	$Lyt\text{-}2^+L3T4^-$ (%)	$Lyt\text{-}2^-L3T4^+$ (%)
Spleen	1/23	0	14.0	N.D.
Normal thymus	1/374†	75.1	3.0	14.5
Tumor 1	1/120	44.5	11.6	19.8
Tumor 2	1/85	45.1	15.2	9.5
Tumor 3	1/266	78.9	3.5	8.9

* Frequencies were calculated by limiting dilution analysis. See Materials and Methods.
† An average value from several previous experiments.

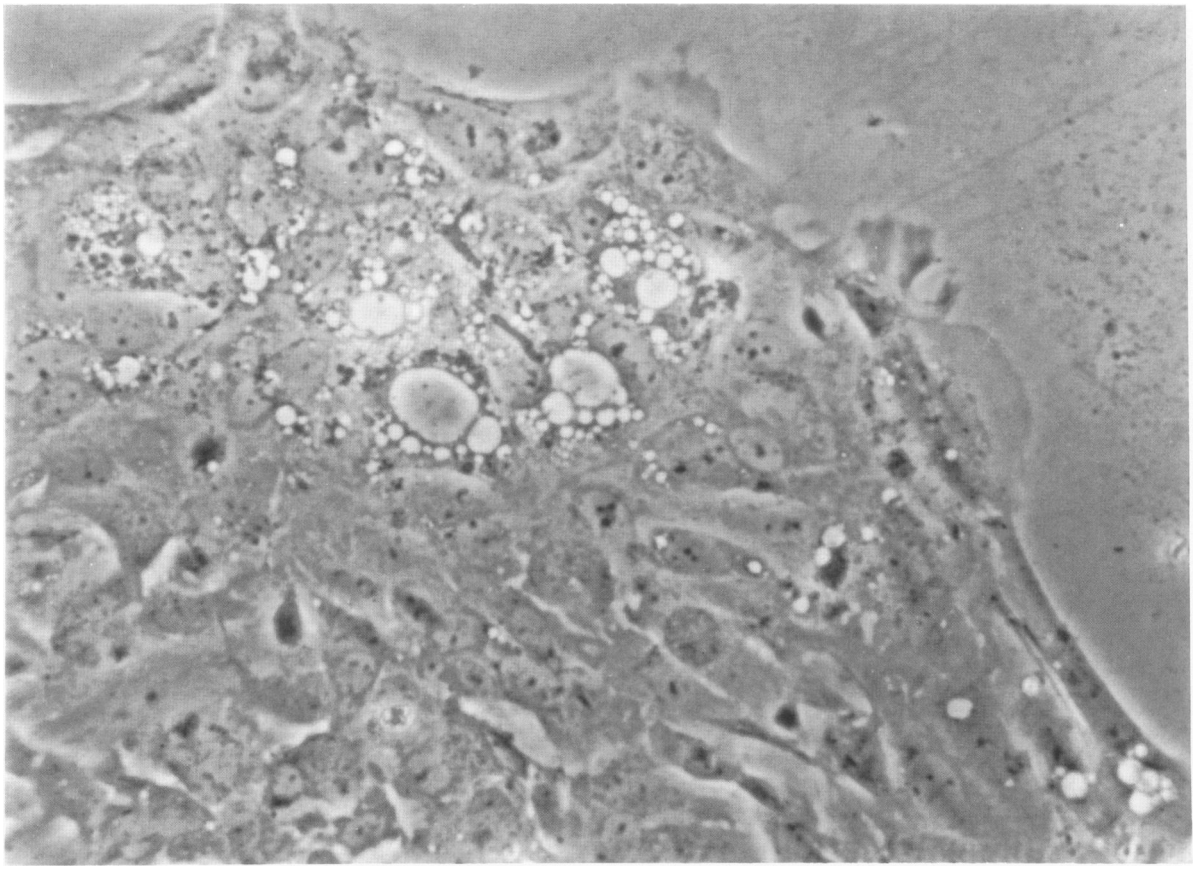

Figure 7. *Polyoma-induced thymic epithelial tumor fragments were grown in tissue culture with 5% CO_2 at 37 C for 2-to-3 weeks. This photomicrograph with a Leitz inverted phase contrast microscope illustrates the epithelial characteristics of an adherent outgrowth from an explant* in vitro.

mice infected with the SV-10 strain of Py at birth. Immunologic restoration was measured by prevention of a wasting syndrome, improvement of animal survival, and the ability to produce antibodies to sheep erythrocytes. Vandeputte, however, was unable to demonstrate restoration of immunologic competence in neonatally thymectomized mice implanted with a thymic tumor, again generated using a thymotropic strain of Py in C3H mice.[27]

In the present study, we partially characterized both the neoplastic epithelial component and the normal lymphoid component in Py virus (strain PTA-5)-induced thymic tumors that arise in C3H/Bittner mice after neonatal infection with the virus. This particular model has an advantage over other possible approaches for examining thymic epithelial tumors because of the efficiency with which this virus causes thymic tumors in C3H/Bittner mice ie, approximately one half of the animals infected at birth will eventually develop thymic tumors.

These murine tumors are similar to the epithelium-predominant, spindle cell thymomas described in humans. The epithelial origin of the tumors was confirmed by the identification of tonofilaments and desmosomes at the ultrastructural level and by the strong staining reactions of tumor sections with an anti-cytokeratin MAb. Also, as do all normal thymic epithelium, the tumor cells express Class II MHC molecules.

We were interested initially in determining whether neoplastic transformation was involving the cortical epithelium, medullary epithelium, or both. Staining of tumor sections through immunoperoxidase for a murine thymic cortical epithelium-specific marker, ER-TR4, and a murine thymic medullary epithelium-specific marker, ER-TR5, showed extreme heterogeneity of staining. Of interest, areas of the tumors that appeared to be homogeneous by routine H&E staining showed heterogeneity when stained with ER-TR4 and ER-TR5 MAbs, in addition to anti-asialo-GM_1, which stains all normal medullary epithelium. There are two basic assumptions that may or may not be valid regarding assignment of clonality with the ER-TR4 and ER-TR5 markers. These assumptions are that the markers are stably expressed after neoplastic transformation and that the cells are not capable of coexpressing these markers. In fact, there are many examples of heterogeneous expression of cell surface antigens in normal tissues and their neoplastic counterparts.[65] Further, one epitope found on normal human thymic epithelium is not ex-

pressed in human epithelial tumors.[66] Therefore, we reviewed our own results with caution and did not assign either a cortical or a medullary origin to the tumors.

Although the tumors contained variable numbers of lymphocytes, the overall lymphoid density, as measured by the cellularity index of the tumors, was less than in normal thymus. Scattered in the tumors were islands of Lyt-2$^+$ lymphocytes supported by a normal appearing dendritic network of Ia$^+$, cytokeratin$^+$, ER-TR4$^+$, ER-TR5$^-$ epithelial cells. Such "cortical islands" generally appeared at the periphery of the tumors in association with the tumor capsule; this suggested that, as the tumors expanded, normal cortical remnants were pushed peripherally. Remnants of normal medullary tissue were scarce, indicating that the growing tumors disrupted medullary architecture. Individual lymphocytes were scattered throughout the epithelial-predominant regions suggesting that the tumor mass represented a medullary microenvironment.

The lymphocytes in the tumors appeared to be normal thymic lymphocytes, rather than an infiltrate of mature T cells. Most lymphocytes had a cortical phenotype, being Tdt$^+$, PNA$^+$, Lyt-2$^+$, L3T4$^+$, Thy1.2^{bright}, H-2K$^{k\,dim}$, Lyt-1^{dim}, ThB$^+$, and J11d$^+$. However, the more mature medullary phenotype was more abundant in the tumors than in the normal thymus, as demonstrated by two-color immunofluorescence staining for L3T4 and Lyt-2. This probably explains the increased frequency of responsiveness to Con A plus IL-2 among tumor lymphocytes as compared with normal thymocytes. Consistent with the present findings, human thymic epithelial tumors have a greater frequency of lymphocytes capable of proliferating in response to polyclonal T cell mitogens than does the normal human thymus.[63,67,68] In studies to be presented elsewhere, we will show that similar Py virus-induced epithelial tumors can continue to have thymic function when serially transplanted (Harrod and Kettman, submitted for publication).

References

1. Kyewski BA: Seeding of thymic microenvironments defined by distinct thymocyte-stromal cell interactions is developmentally controlled. J Exp Med 1987, 166:520–528
2. Kyewski BA, Rouse RV, Kaplan HS: Thymocyte rosettes: Multicellular complexes of lymphocytes and bone marrow derived stromal cells in the mouse. Proc Natl Acad Sci USA 1982, 79:5646–5650
3. Wekerle H: Thymic nurse cells. Ia-bearing epithelium involved in T lymphocyte differentiation? Nature 1980, 283: 402–404
4. Kruisbeek AM, Bridges S, Carmen J, Longo DL, Mond JJ: *In vivo* treatment of neonatal mice with anti-I-A antibodies interferes with the development of the class I, class II, and M1s-reactive proliferating T cell subset. J Immunol 1985, 134:3597–3604
5. Tridente G: Immunopathology of the human thymus. Semin Hematol 1985, 22:56–67
6. Scollay R, Shortman K: Identification of early stages of T lymphocyte development in the thymus cortex and medulla. J Immunol 1985, 134:3632–3642
7. Hiai H, Nishi Y, Miyazawa T, Matsudaira Y, Nishizuka Y: Mouse lymphoid leukemias: Symbiotic complexes of neoplastic lymphocytes and their microenvironments. J Natl Cancer Inst 1981, 66:713–722
8. Duijvestijn AM, Sminia T, Kohler YG, Janse EM, Hoefsmit EC: Ontogeny of the rat thymic microenvironment: Development of the interdigitating cell and macrophage populations. Dev Comp Immunol 1984, 8:451–460
9. Singer A, Hatcock KS, Hodes RJ: Self recognition in allogeneic thymic chimeras: Self recognition by T helper cells from thymus engrafted nude mice is restricted to the thymic H-2 haplotype. J Exp Med 1982, 155:339–344
10. Duijvestijn AM, Barclay AN: Identification of the bone marrow-derived Ia positive cells in the rat thymus: A morphological and cytochemical study. J Leukocyte Biol 1984, 36:561–568
11. Zinkernagel RM, Callahan GM, Althage A, Cooper S, Klein PA, Klein H: On the thymus in the differentiation of H-2 self recognition by T cells: Evidence for clonal recognition. J Exp Med 1978, 147:882–896
12. Haynes BF, Scearce RM, Lobach DF, Hensley LL: Phenotypic characterization and ontogeny of mesodermal-derived and endocrine epithelial components of the human thymic microenvironment. J Exp Med 1984, 159:1149–1168
13. deMaagd RA, Mackenzie WA, Schuurman H-J, Ritter MA, Price KM, Broekhuizen R, Kater L: The human thymus microenvironment: heterogeneity detected by monoclonal anti-epithelial cell antibodies. Immunol 1985, 54:745–754
14. Haynes BF, Warren RW, Buckley RH, McClure JE, Goldstein AL, Henderson FW, Hensley LL, Eisenbarth GS: Demonstration of abnormalities in expression of thymic epithelial surface antigens in severe cellular immunodeficiency diseases. J Immunol 1983, 130:1182–1188
15. van Vliet E, Melis M, van Ewijk W: Monoclonal antibodies to stromal cell types of the mouse thymus. Eur J Immunol 1984, 14:524–529
16. McFarland EJ, Scearce RM, Haynes BF: The human microenvironment: Cortical thymic epithelium is an antigenically distinct region of the thymic microenvironment. J Immunol 1984, 133:1241–1249
17. van Ewijk W: Immunohistology of lymphoid and non-lymphoid cells in the thymus in relation to T lymphocyte differentiation. Am J Anat 1984, 170:311–330
18. Rosai J: "Lymphoepithelioma-like" thymic carcinoma: Another tumor related to Epstein-Barr virus? New Engl J Med 1985, 312:1320–1322
19. Boeckman DE, Stutman O: Fine structure of a transplanted chemically induced non-lymphoid thymoma. Cancer Res 1969, 29:1663–1668
20. Stutman O, Yunis EJ, Good RA: Carcinogen induced tumors of the thymus. I. Restoration of neonatally thymectomized

mice with a functional thymoma. J Natl Cancer Inst 1968, 41:1431–1452

21. Stutman O, Yunis EJ, Good R: Carcinogen-induced tumors of the thymus. II. Lung colonies as a means of separating different cell types of a functional thymoma. J Natl Cancer Inst 1969, 42:783–795
22. Stutman O, Yunis EJ, Good RA: Carcinogen-induced tumors of the thymus. III. Restoration of neonatally thymectomized mice with thymomas in cell-impermeable chambers. J Natl Cancer Inst 1969, 43:499–508
23. Stutman O, Yunis EJ, Good RA: Carcinogen induced tumors of the thymus. IV. Humoral influence of normal thymus and functional thymomas and influence of post-thymectomy period on restoration. J Exp Med 1969, 133:809–819
24. Chollet P, Plagne R, Fonck Y, Chassagne J, Betail G, Dardenne M, Bach JF: Thymoma with hypersecretion of thymic hormones. Thymus 1981, 3:321–334
25. Mokhtar N, Hsu S-M, Lad RP, Haynes BF, Jaffe ES: Thymoma: Lymphoid and epithelial components mirror the phenotype of normal thymus. Human Pathol 1984, 15:378–384
26. Piantelli M, Ranelletti FO, Musiani P, Lauriola L, Maggiano N: A human thymoma with prothymocyte-like infiltration. Clin Immunol Immunopathol 1983, 28:350–360
27. Vandeputte M: Failure of thymoma grafts to restore the immunological competence in thymectomized mice. Pathol Eur 1967, 2:55–68
28. Rosai J, Levine GD: Atlas of Tumor Pathology. Second Series Facs. 13. Tumors of the Thymus, Washington, DC, Armed Forces Institute of Pathology 1976
29. Stewart SE, Eddy BE, Gochenour AM, Borgese NG, Grubbs GE: The induction of neoplasms with a substance released from mouse tumors by tissue culture. Virol 1957, 3:380–400
30. Stewart SE, Eddy BE, Borgese N: Neoplasms in mice inoculated with a tumor agent carried in tissue culture. J Natl Cancer Inst 1958, 20:1223–1236
31. Buffett RF, Commerford SL, Furth J, Hunter MJ: Agent in AK leukemic tissues, not sedimented at 105,000*g*, causing neoplastic and non-neoplastic lesions. Proc Soc Exp Biol Med 1958, 99:401–407
32. Dawe, CJ, Law LW, Dunn TB: Studies of parotid-tumor agent in cultures of leukemic tissue of mice. J Natl Cancer Inst 1959, 23:717–797
33. Mishell B, Shiigi SM: Selected Methods in Cellular Immunology. San Francisco, WH Freeman and Co. 1980, p 23
34. Horan P, Kappler J: Automated fluorescent analysis for cytotoxicity assays. J Immunol Methods 1977, 18:309–316
35. Dialynas DP, Wilde DB, Marrack P, Pierres A, Wall KA, Havran W, Otton G, Loken MR, Pierres M, Kappler J, Fitch FW: Characterization of the murine antigenic determinant, designated L3T4a, recognized by monoclonal antibody GK1.5: Expression of L3T4a by functional T cell clones appears to correlate primarily with class II MHC antigen reactivity. Immunol Rev 1983, 74:29–56
36. Haskins K, Hannum C, White J, Roehm N, Kubo R, Kappler J, Marrack P: The antigen-specific, major histocompatibility complex-restricted receptor on T cells. VI. An antibody to a receptor allotype. J Exp Med 1984, 160:452–471
37. Ledbetter JA, Herzenberg LA: Xenogeneic monoclonal antibodies to mouse lymphoid differentiation antigens. Immunol Rev 1979, 47:63–90
38. Oi VT, Jones PP, Goding JW, Herzenberg LA, Herzenberg LA: Properties of monoclonal antibodies to mouse Ig allotypes, H-2, and Ia antigens. Curr Top Microbiol Immunol 1978, 81:115–129
39. Forman J, Tonkonogy S, Flaherty L: The Qa-2 subregion controls the expression of two antigens recognized by H-2 unrestricted cytotoxic cells. J Exp Med 1982, 155:749–767
40. Doran TI, Garner LA, Tharp MD: Studies on the pathogenesis of mutilating keratoderma of volwinkel using mouse monoclonal anti-keratin antibodies. J Invest Derm 1986, 86:472
41. Chorney M, Shen F-W, Michaelson J, Boyse EA: Monoclonal antibody to an alloantigenic determinant on Beta 2-microglobulin (β2M) of the mouse. Immunogenet 1982, 16:91–93
42. Yam LT, Li CY, Crosby WH: Cytochemical identification of monocytes and granulocytes. Am J Clin Pathol 1971, 55: 283–291
43. Barka T, Anderson PJ: Methods for acid phosphatase using hexazonium parasanilin as complex. J Histochem Cytochem 1962, 10:741–753
44. Hanker JS, Yates PE, Metz CB, Rustioni A: A new specific sensitive, and non-carcinogenic reagent for the demonstration of horse radish peroxidase. Histochem J 1977, 9:789–792
45. Kettman JR, Soederberg A, Lefkovits I: Mitogenic activation of B cells *in vitro:* The properties of adherent accessory cells as revealed by partition analysis. J Immunol 1986, 137: 1144–1148
46. Battifora H, Sun T-T, Bahu RM, Rao S: The use of antikeratin antiserum as a diagnostic tool: Thymoma versus lymphoma. Human Pathol 1980, 11:635–641
47. Van Ewijk W, Rouse RV, Weissman IL: Distribution of H-2 microenvironments in the mouse thymus: Immunoelectron microscopic identification of I-A and H-2K bearing cells. J Histochem Cytochem 1980, 28:1089–1099
48. Charley MR, Mikhael A, Hoot G, Hackett J, Bennett M: Studies addressing the mechanism of anti-asialo GM_1 prevention of graft-versus-host disease due to minor histocompatibility antigenic differences. J Invest Derm 1985, 85:1215–1235
49. Duijvestijn AM, Kohler YG, Hoefsmit ECM: Interdigitating cells and macrophages in the acute involuting rat thymus. Cell Tissue Res 1982, 224:291–301
50. Milicevic NM, Milicevic ZJ: Enzyme-histochemical characterization of macrophages in the rat thymus, with special reference to metallophilic cells of the corticomedullary zone. J Leukocyte Biol 1984, 36:761–769
51. Manconi PE, Ennas MG, Paghi L, Tedde A, Bistrusso A, Masia G, Costa G: Alpha-naphthyl acetate esterase activity in mouse thymus and other lymphoid organs. Thymus 1982, 4:135–146
52. Smith C: Studies on thymus of the mammal. IX. Histochemical study of irradiated mouse thymus. Proc Soc Exp Biol Med 1956, 93:310–314
53. Smith C: Studies on the thymus of the mammal. XIV. Histology and histochemistry of embryonic and early postnatal

thymuses of C57BL/6 and AKR strain mice. Am J Anat 1965, 116:611–630
54. van Ewijk W, van Soest PL, van den Engh GJ: Fluorescence analysis and anatomic distribution of mouse T lymphocyte subsets defined by monoclonal antibodies to the antigens Thy-1, Lyt-1, Lyt-2, and T-200. J Immunol 1981, 127:2594–2604
55. Scollay R, Shortman K: Thymocyte subpopulations: An experimental review, including flow cytometric cross-correlations between the major murine thymocyte markers. Thymus 1983, 5:245–295
56. Micklem HS, Ledbetter JA, Eckhardt LA, Herzenberg LA: Analysis of lymphocyte subpopulations with monoclonal antibodies to Thy-1, Lyt-1, Lyt-2, and ThB antigens, Regulatory T Lymphocytes. Edited by B Perris, HJ Vogel. New York, Academic Press 1980, pp 245–294
57. Mathieson BJ, Fowlkes BJ: Cell surface antigen expression on thymocytes: Development and phenotypic differentiation of intrathymic subsets. Immunol Rev 1984, 82:141–173
58. Bruce J, Symington FW, McKean TJ, Sprent J: A monoclonal antibody discriminating between subsets of T and B cells. J Immunol 1981, 127:2496–2501
59. Goldschneider I, Gregoire KE, Barton RW, Bollum F: Terminal deoxynucleotidyl transferase in thymocytes demonstrated by immunofluorescence. Proc Natl Acad Sci USA 1977, 74:734–738
60. Salyer WR, Eggleston JC: Thymoma: A clinical and pathological study of 65 cases. Cancer 1976, 37:229–249
61. Chilosi M, Menestriano F, Iannucci AM, Fiore-Donati L, Pizzolo G, Janossy G: Immunohistochemical analysis of thymoma: Evidence for medullary origin of epithelial cells. Am J Surg Pathol 1984, 8:309–318
62. Wada BA, Bain K, Salm TV: The phenotype of lymphocytes in a thymoma as studied with monoclonal antibodies. Clin Immunol Immunopathol 1984, 30:1197–1201
63. Lauriola L, Musiani P, Ranelletti O, Maggiano N, Paintelli M: Human thymoma lymphocyte mitogenesis: Glucocorticoid inhibitory capacity as function of the size of the more mature T cell subset. Clin Exp Immunol 1983, 52:477–484
64. Law LW, Dunn TB, Trainin N, Levey RH: Studies of thymic function. Wistar Institute Symposium, Monograph No. 2. Philadelphia, Wistar Institute Press 1964, pp 105–120
65. Edwards PAW: Heterogeneous expression of cell surface antigens in normal epithelia and their tumours, revealed by monoclonal antibodies. Br J Cancer 1985, 51:149–160
66. Savino W, Berrih S, Dardenne M: Thymic epithelial antigen, acquired during ontogeny and defined by the anti-p19 monoclonal antibody, is lost in thymomas. Lab Invest 1984, 51:292–296
67. Lauriola L, Maggiano N, Marino M, Carbone A, Piantelli M, Musiani P: Human thymoma: Immunologic characteristics of the lymphocytic component. Cancer 1981, 48:1992–1995
68. Musiani P, Lauriola L, Maggiano N, Tonali P, Piantelli M: Functional properties of human thymoma lymphocytes: Role of subcellular factors in blastic activation. J Natl Cancer Inst 1982, 69:827–831

Acknowledgment

We thank Drs. Michael Bennett and Florence Harrod for manuscript review, Ms. Ann Buser for her technical expertise on the operation of the Ortho Cytofluorograph, Ms. Bettye Joe Washington for secretarial expertise, and especially Dr. Clyde J. Dawe for providing viral seed, words of encouragement, and for manuscript review.